This article was downloaded by:
On: *14 January 2011*
Access details: *Access Details: Free Access*
Publisher *Taylor & Francis*
Informa Ltd Registered in England and Wales Registered Number: 1072954 Registered office: Mortimer House, 37-41 Mortimer Street, London W1T 3JH, UK

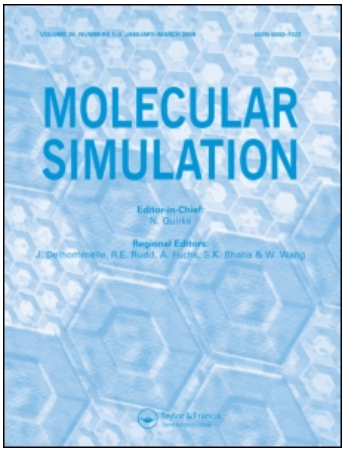

Molecular Simulation
Publication details, including instructions for authors and subscription information:
http://www.informaworld.com/smpp/title~content=t713644482

Computational study of simple and water-assisted tautomerism of 1,3-oxazine-4,6-diones and 1,3-thiazine-4,6-diones

H. Tavakol[a]
[a] Department of Chemistry, University of Zabol, Zabol, Iran

Online publication date: 16 April 2010

To cite this Article Tavakol, H.(2010) 'Computational study of simple and water-assisted tautomerism of 1,3-oxazine-4,6-diones and 1,3-thiazine-4,6-diones', Molecular Simulation, 36: 5, 391 — 402
To link to this Article: DOI: 10.1080/08927020903530963
URL: http://dx.doi.org/10.1080/08927020903530963

PLEASE SCROLL DOWN FOR ARTICLE

Full terms and conditions of use: http://www.informaworld.com/terms-and-conditions-of-access.pdf

This article may be used for research, teaching and private study purposes. Any substantial or systematic reproduction, re-distribution, re-selling, loan or sub-licensing, systematic supply or distribution in any form to anyone is expressly forbidden.

The publisher does not give any warranty express or implied or make any representation that the contents will be complete or accurate or up to date. The accuracy of any instructions, formulae and drug doses should be independently verified with primary sources. The publisher shall not be liable for any loss, actions, claims, proceedings, demand or costs or damages whatsoever or howsoever caused arising directly or indirectly in connection with or arising out of the use of this material.

Molecular Simulation
Vol. 36, No. 5, April 2010, 391–402

Taylor & Francis
Taylor & Francis Group

Computational study of simple and water-assisted tautomerism of 1,3-oxazine-4,6-diones and 1,3-thiazine-4,6-diones

H. Tavakol*

Department of Chemistry, University of Zabol, Zabol, Iran

(*Received 5 August 2009; final version received 4 December 2009*)

Density functional theory (DFT) calculations are applied to optimise the structure of three possible tautomers of some 5H-1,3-oxazine-4,6-diones and 5H-1,3-thiazine-4,6-diones and their transition states using B3LYP/6-311++G** level of theory. Then, important molecular parameters, IR frequencies and energetic parameters are calculated. In all cases, tautomer **2** is about 0.7–8.7 kcal/mol more stable than tautomer **1** and about 10.4–14.4 kcal/mol more stable than tautomer **3**. Our results confirm the available experimental data approving the higher stability of tautomer **2**. Furthermore, barrier energies and reaction rate constants of the hydrogen exchange between each pair of tautomers in the presence of one, two and three water molecules are calculated. The computed activation barriers in the presence of water molecules are about 23.8–76.2 kcal/mol lower than those in the gas phase.

Keywords: tautomerism; oxazinedione; thiazinedione; transition state; water assisted

Downloaded At: 17:10 14 January 2011

1. Introduction

Oxazinones, thiazinones and their derivatives constitute an important group of heterocycles, which has attracted interest due to their significant role in biological reactions [1]. In recent years, much attention has been focused on the study of these compounds since the discovery of their application in the synthesis of anti-HIV drug [2]. Furthermore, they have shown diverse pharmacological properties such as progesterone receptor antagonist [3], antitumour [4], antiviral [5], antithrombotic [6], antimicrobacterial [7], anti-inflammatory [8], anti-diabetic and hypolipidaemic [9] effects. Oxazinones have also been utilised as useful synthetic precursors for the preparation of some organic compounds [10–12] and metal complexes [13].

5H-1,3-Oxazine-4,6-diones (OZDs) and 5H-1,3-thiazine-4,6-diones (TZDs) also have anti-inflammatory and antimicrobacterial activities [14–20]. They can be used in the synthesis of very useful compounds such as α-amino acids [21]. Because of the importance of the title compounds, OZDs and TZDs have been the subject of some studies including the study of their anomeric effect [22], reduction [23], ring contraction [24] and application in DNA chemistry [25].

Since tautomerism in the OZD and TZD structures affects their chemical and biological activities, especially their diverse pharmacological properties [3,7], it is very important to learn about the complete scheme of tautomerism and the reaction path between different tautomers. In this line, the effect of substituents and, more importantly, the effect of solvent on this tautomerism interconversion should also be worked out clearly. Moreover, despite a large number of published reports about the study of tautomerism in different compounds [26–38], the study of tautomerism in OZDs or TZDs has not been reported. Therefore, the relative importance of different tautomers and their interconversion can be studied in detail. Another important feature of these compounds that has not received much attention is the study of intermolecular tautomerism. This type of study is one of the important topics in recent computational reports [39–41].

In this work, structural, bonding and vibrational properties (Tables 5 and 6) and tautomerism in the OZD, TZD, mono- and dimethyl derivatives (Figure 1, **a**–**h**) and their transition states (Table 2) are studied using DFT-B3LYP/6-311++G** calculations (Tables 1–4; Figures 3 and 4). Furthermore, the intermolecular tautomerism interconversion and reaction path for one of them (molecule **e**) are also obtained in the presence of one, two and three water molecules (Tables 7 and 8). Details of computations and the results obtained in this work are presented below.

2. Methods

Density functional theory (DFT) has been widely applied by chemists to study the electronic structure of molecules in the past 30 years [42,43]. In this work, all calculations have been carried out at the B3LYP/6-311++ G** level

*Emails: h_tavakol@uoz.ac.ir; hosein_ta@yahoo.com

ISSN 0892-7022 print/ISSN 1029-0435 online
© 2010 Taylor & Francis
DOI: 10.1080/08927020903530963
http://www.informaworld.com

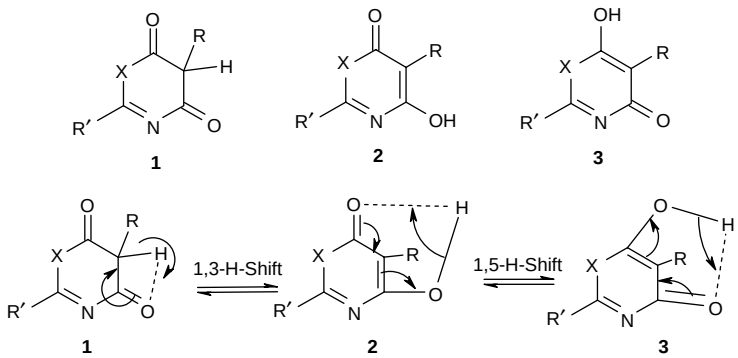

	R	R′	X
a	H	H	S
b	H	Me	S
c	Me	H	S
d	Me	Me	S
e	H	H	O
f	H	Me	O
g	Me	H	O
h	Me	Me	O

Figure 1. Three possible tautomers of selected compounds with representation of both '1,3' and '1,5' hydrogen shifts.

of theory [44,45]. The B3LYP method has been validated to give results similar to those of the more computationally expensive MP2 theory for molecular geometry and frequency calculations [46,47]. Gaussian 03 [48] and GaussView 03 [49] program packages have been employed for computing and visualising the desired properties. The absence of imaginary frequencies verified that the structures were true minima at their respective levels of theory for each tautomer. Furthermore, in each pair of tautomers, stationary point geometry with one imaginary frequency has been found and the transition state has been identified using Schlegel's synchronous-transit-guided quasi-Newton (QST3) [50,51] method started from the fully optimised structure of one tautomer and finished on the fully optimised structure of another tautomer. Intrinsic reaction coordinate calculations proved that each reactant linked to the correct product via allocated transition state. Calculations of the rate constants and reaction dynamic have been carried out using canonical transition state theory applying the Eyring equation [52–54]. IR frequencies and energies obtained from the frequency calculations were used after applying the appropriate scaling factor (both of them scaled by 0.967; http://cccbdb.nist.gov/vibscalejust.asp). Free energies of solvation for all structures were calculated using SCRF keyword with Tomasi's polarised continuum model (PCM) [55,56] at the B3LYP/6-311++G** level of theory. Four different solvents (cyclohexane, chloroform, acetone and DMSO) with different dielectric constants (respectively, 2.02, 4.90, 20.70 and 46.70) have been used.

3. Results and discussion

This work was started with eight different structures of OZDs and TZDs. In Figure 1, the structures of all tautomers in eight selected structures are shown. Structures **a**–**d** are TZDs and the other structures (**e**–**h**) are OZDs. According to this figure, three tautomers (**1**–**3**) can exist for each structure. Spectroscopic data of previous report showed that the major product obtained from the synthesis of some OZDs and TZDs is tautomer **2** [14]. Figure 1 also shows that the interconversions of tautomers **1** to **2** and **1** to **3** are similar to '1,3' hydrogen shift and the interconversion of tautomers **2** to **3** is similar to '1,5' hydrogen shift.

For more simplicity, geometric (*cis–trans* and *syn–anti*) and conformational isomers were neglected in this study. Therefore, only possible tautomers have been considered in the calculations. Concluding, these structures were employed without any symmetry restriction, pre-defined geometric or conformational structures, and *C*1 symmetry was assumed for all structures.

3.1 Optimised structures

Molecular structures of the optimised (final) tautomers and transition states are shown in Tables 1 and 2, respectively.

According to the above tables, optimised structures of tautomers **2** and **3** are completely planar, the structure of tautomer **1** is half-chair or envelope-like with about 15° deviation from the plane, the structure of TS1 (the transition state between tautomers **1** and **2**) is half-chair with about 20° deviation from the plane, the structure of TS2 (the transition state between tautomers **1** and **3**) has a planar ring and slightly spatial ring substituents and the structure of TS3 (the transition state between tautomers **2** and **3**) is completely envelope-like with 36–42° deviation from the plane.

3.2 Molecular parameters

Calculated molecular parameters for optimised structures are listed in Table S1 of the Supplementary Material. The numbering schemes of all molecules are the same as the pre-defined numbers for each atom as shown in Tables 1 and 2. This numbering scheme (Figure 2) can be applied identically for all tautomers and transition states. In Figure 2, only similar numbers of all structures are shown.

Downloaded At: 17:10 14 January 2011

Table 1. Final structure of the optimised tautomers.

Molecule	Tautomer **1**	Tautomer **2**	Tautomer **3**
a	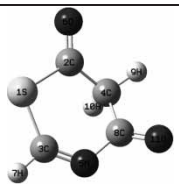	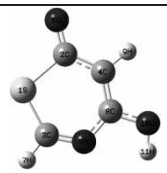	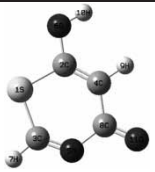
b	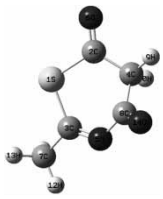	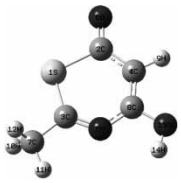	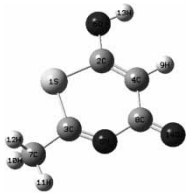
c	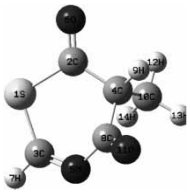		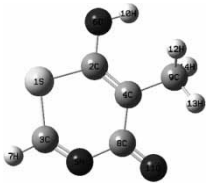
d		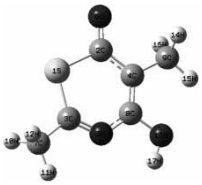	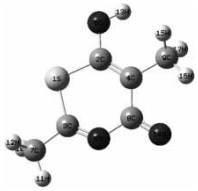
e	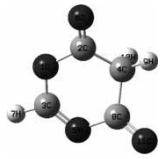	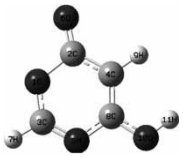	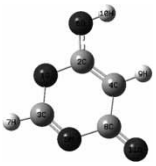
f	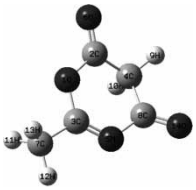	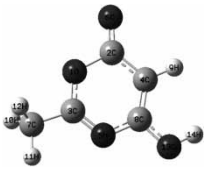	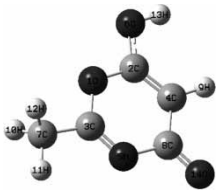
g	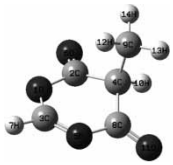		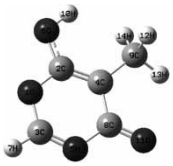
h			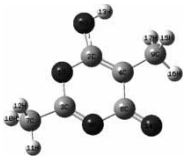

Downloaded At: 17:10 14 January 2011

Table 2. Final structure of the optimised transition states.

Molecule	TS1 (between tautomers **1** and **2**)	TS2 (between tautomers **1** and **3**)	TS3 (between tautomers **2** and **3**)
a	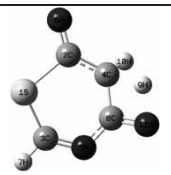	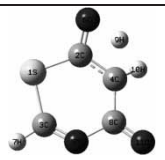	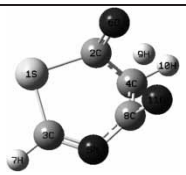
b	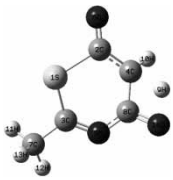		
c	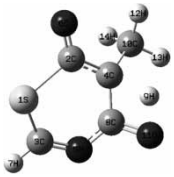	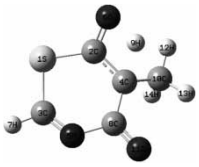	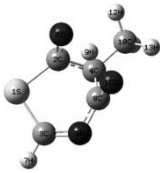
d			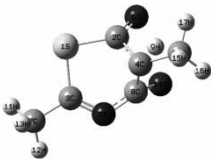
e	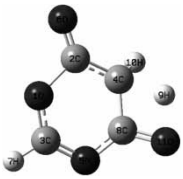	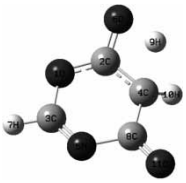	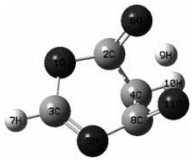
f	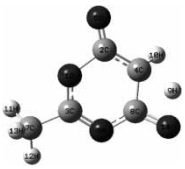	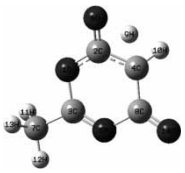	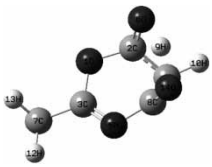
g	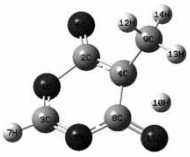	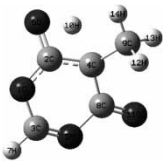	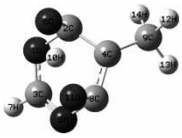
h	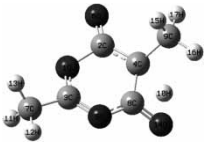	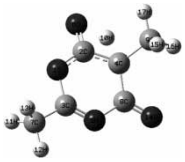	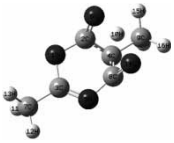

Downloaded At: 17:10 14 January 2011

Table 3. Kinetic and thermodynamic data of all tautomers and transition states.[a]

Molecule	$\Delta H(1-2)$[b]	$\Delta H(3-2)$[b]	$\Delta G(1-2)$[c]	$\Delta G(3-2)$[c]	K_{eq} $(1-2)$[d]	K_{eq} $(3-2)$[d]
a	−5.6	−13.7	−5.1	−13.4	5.9×10^3	6.2×10^9
b	−4.6	−13.5	−4.8	−13.0	3.4×10^3	3.1×10^9
c	−8.0	−13.6	−8.7	−13.4	2.2×10^6	6.8×10^9
d	−6.9	−13.4	−8.0	−13.0	6.9×10^5	3.4×10^9
e	−1.6	−10.6	−1.1	−10.4	6.5	4.2×10^7
f	−1.0	−10.9	−0.7	−10.7	3.1	7.0×10^7
g	−8.4	−14.3	−8.6	−14.0	2.1×10^6	2.0×10^{10}
h	−7.8	−14.5	−8.2	−14.4	9.5×10^5	3.4×10^{10}
	$\Delta G^{\#}(2-\text{ts1})$[e]	$\Delta G^{\#}(1-\text{ts2})$[e]	$\Delta G^{\#}(2-\text{ts3})$[e]	$k(2-1)$[f]	$k(1-3)$[f]	$k(2-3)$[f]
a	55.7	62.6	91.3	9.7×10^{-29}	8.7×10^{-34}	7.7×10^{-55}
b	54.9	62.4	91.1	3.3×10^{-28}	1.1×10^{-33}	9.7×10^{-55}
c	60.5	65.2	92.7	2.6×10^{-32}	1.0×10^{-35}	6.8×10^{-56}
d	59.5	65.1	92.3	1.5×10^{-31}	1.1×10^{-35}	1.3×10^{-55}
e	55.1	64.7	93.8	2.4×10^{-28}	2.4×10^{-35}	1.0×10^{-56}
f	54.4	64.8	93.3	8.9×10^{-28}	2.1×10^{-35}	2.6×10^{-56}
g	71.6	66.6	98.4	2.1×10^{-40}	1.0×10^{-36}	4.9×10^{-60}
h	63.2	66.6	97.9	3.0×10^{-34}	9.1×10^{-37}	1.1×10^{-59}

Note: The reference for all differences is the most stable compound.[a] All ΔH and ΔG values were reported in kcal/mol and rate constants were reported in s^{-1}. [b] $\Delta H(n-m) =$ Enthalpy of tautomer $m(Hm)$ − Enthalpy of tautomer $n(Hn)$. [c] $\Delta G(n-m) =$ Gibbs free energy of tautomer $m(Gm)$ − Gibbs free energy of tautomer $n(Gn)$. [d] $K_{eq}(n-m)$: the ratio of $[m]/[n]$, obtained from $K_{eq} = \exp(-\Delta G(n-m)/RT)$. [e] $\Delta G^{\#}(n-\text{ts1}) =$ Gibbs free energy of ts1 (Gts1) − Gibbs free energy of tautomer $n(Gn)$. [f] $k(n-m)$: the reaction rate for conversion of n to m.

Downloaded At: 17:10 14 January 2011

The X_1—C_2 bond lengths in molecules **a**–**d** lie between 1.7 and 1.9 Å. Its length is exactly 1.8 Å in tautomers **1** and **3**, and TS3, 1.9 Å in tautomer **2** and TS1 and 1.7 Å in TS2 in all optimised TZDs. In addition, its length is 1.4 Å in tautomers **1** and **2** and TS3, 1.3 Å in tautomer **3** and TS2, and 1.5 Å in TS1 in calculated OZDs. Higher atomic radius of sulphur vs. oxygen is responsible for the greater value of the X_1—C_2 bond length in molecules **a**–**d**. The bond lengths of C_3—N_5 and C_3—H_7 (or C_3—C_7) in OZDs have the same value as those in TZDs. In addition, the length of the C_2—O_6 bond lies between 1.2 and 1.4 Å, and the C_4—C_8 bond length lies between 1.4 and 1.5 Å.

Observing bond angle variations, hybridisation changes in the central atom of each angle can be followed. In molecules **a**–**d**, C_2—X_1—C_3 bond angles in tautomers **1** and **2**, and TS1 are more than 100°, and those in TS2, and TS3 and tautomer **3** are less than 100°. C_2—X_1—C_3 and X_1—C_2—C_4 angles in molecules **e**–**h** are in general larger than those in molecules **a**–**d**. X_1—C_2—O_6, C_4—C_2—O_6 and X_1—C_3—N_5 angles have expected values according to the hybridisation of their central atom.

The planarity of molecules can be followed by dihedral angles. For example, in tautomers **2** and **3**, C_3—X_1—C_2—C_4, C_2—X_1—C_3—N_5 and X_1—C_2—C_4—C_8 dihedral angles are near 0° and C_3—X_1—C_2—O_6 and C_2—X_1—C_3—H_7 dihedral angles are near 180°, thus all of these angles confirm the planarity of the corresponding tautomers. Following this, in all structures, the value of the deviation of this dihedral angle from 0° (or 180°) is a criterion of the deviation rate from the planar structure.

3.3 Kinetic and thermodynamic data

In Table 3, Gibbs free energies and other important thermodynamic and kinetic data for all structures at 298.15 K and 1 atmosphere pressure are presented. All equilibrium constants for tautomeric interconversion were calculated using $\Delta G = -RT \ln K_{eq}$.

The data presented in Table 3 show that tautomer **2** is most stable, followed by tautomer **1**, and tautomer **3** is least stable in all computed OZDs and TZDs. The difference between Gibbs free energies for tautomers **1** and **2** (Gibbs free energy of tautomer **2** (the most stable tautomer) minus Gibbs free energy of tautomer **1**) lies between −0.7 and −8.7 kcal/mol and for tautomers **3** and **2** (Gibbs free energy of tautomer **2** (the most stable tautomer) minus Gibbs free energy of tautomer **3**) lies between −10.4 and −14.4 kcal/mol. The differences between tautomers **1** and **2** in molecules **e** and **f** are smaller than those in the other molecules. This observation can be the subject of further investigation. Moreover, the value of the equilibrium constant (obtained from Gibbs free energies) for the conversion of tautomer **1** to **2** (the most stable tautomer) lies between 3.1 and 2.2×10^6 and the equilibrium constant for the conversion of tautomer **3** to **2** (the most stable tautomer) lies between 4.2×10^7 and 3.4×10^{10}.

The effects of the substituent were also studied. The thermodynamic results show that the addition of the methyl substituent at the C4 position (between two carbonyl groups) causes the increase in the relative stability of tautomer **2** vs. **1** because the absolute values of ΔG between these two tautomers in molecules **c**, **d**, **g** and **h** (i.e. all of them have methyl at C4) were increased. This phenomenon

Downloaded At: 17:10 14 January 2011

Table 4. Solvation effects with kinetic and thermodynamic data in solvent for all molecules at B3LYP/6-311++G** level of theory.[a]

Solvent	Molecules	Molecules							
		a	**b**	**c**	**d**	**e**	**f**	**g**	**h**
ΔG solvation in acetone	Tautomer **1**	−5.4	−5.5	−4.3	−4.3	−5.9	−6.2	−4.8	−5.0
	Tautomer **2**	−5.0	−5.0	−4.5	−4.5	−7.4	−7.1	−4.9	−4.9
	Tautomer **3**	−8.5	−8.3	−6.8	−6.5	−8.9	−8.8	−7.1	−7.5
	TS1	−4.6	−4.6	−3.4	−3.3	−4.9	−5.0	−3.7	−4.1
	TS2	−6.2	−5.3	−5.1	−4.8	−5.8	−5.8	−5.2	−5.2
	TS3	−2.8	−3.0	−2.9	−2.9	−2.9	−3.2	−2.8	−3.0
ΔG solvation in cyclohexane	Tautomer **1**	−3.4	−3.5	−2.8	−2.7	−3.3	−3.5	−2.7	−2.8
	Tautomer **2**	−3.5	−3.5	−3.4	−3.4	−3.9	−4.0	−3.1	−3.3
	Tautomer **3**	−4.8	−4.8	−4.2	−4.3	−4.6	−4.7	−3.9	−4.2
	TS1	−3.2	−3.4	−2.6	−2.6	−3.0	−3.2	−2.4	−2.7
	TS2	−3.9	−3.4	−3.3	−3.3	−3.3	−3.5	−3.0	−3.1
	TS3	−2.3	−2.8	−2.7	−2.7	−2.2	−2.5	−2.5	−2.6
ΔG solvation in chloroform	Tautomer **1**	−3.4	−3.4	−2.4	−2.2	−3.8	−3.9	−2.8	−2.8
	Tautomer **2**	−3.2	−3.0	−2.6	−2.4	−4.8	−4.5	−2.8	−2.7
	Tautomer **3**	−5.7	−5.4	−4.2	−3.9	−6.0	−5.7	−4.5	−4.5
	TS1	−2.8	−2.7	−1.6	−1.4	−3.0	−2.9	−2.1	−2.0
	TS2	−4.0	−3.1	−2.9	−2.5	−3.6	−3.5	−2.9	−2.8
	TS3	−1.6	−1.5	−1.4	−1.3	−1.7	−1.6	−1.4	−1.3
ΔG solvation in DMSO	Tautomer **1**	−5.0	−5.0	−3.6	−3.4	−5.5	−5.7	−4.1	−4.2
	Tautomer **2**	−4.7	−4.4	−4.0	−3.8	−7.1	−6.7	−4.3	−4.2
	Tautomer **3**	−8.3	−7.9	−6.4	−5.9	−8.7	−8.4	−6.7	−6.9
	TS1	−4.2	−4.0	−2.7	−2.4	−4.5	−4.4	−3.0	−3.3
	TS2	−5.9	−4.3	−4.5	−4.0	−5.4	−5.3	−4.6	−4.4
	TS3	−2.5	−2.4	−2.3	−2.2	−2.4	−2.6	−2.3	−2.3
Thermodynamic and kinetic data in solvent									
Acetone	$K_{eq}(1-2)^b$	3.1×10^{3}	1.3×10^{3}	3.2×10^{6}	9.9×10^{5}	7.5×10^{1}	1.4×10^{1}	2.4×10^{6}	7.4×10^{5}
	$K_{eq}(3-2)^b$	1.7×10^{7}	1.2×10^{7}	1.4×10^{8}	1.1×10^{8}	3.0×10^{6}	4.2×10^{6}	4.4×10^{8}	4.4×10^{8}
	$k(2-1)^c$	4.7×10^{-29}	1.8×10^{-28}	4.2×10^{-33}	2.0×10^{-32}	3.8×10^{-30}	2.6×10^{-29}	2.9×10^{-41}	8.6×10^{-35}
	$k(1-3)^c$	3.3×10^{-33}	7.8×10^{-34}	4.5×10^{-35}	2.7×10^{-35}	2.0×10^{-35}	1.0×10^{-35}	2.1×10^{-36}	1.1×10^{-36}
	$k(2-3)^c$	1.8×10^{-56}	3.5×10^{-56}	4.9×10^{-57}	1.0×10^{-56}	5.4×10^{-60}	3.5×10^{-59}	1.5×10^{-61}	4.5×10^{-61}
Cyclohexane	$K_{eq}(1-2)^b$	6.8×10^{3}	3.4×10^{3}	6.0×10^{6}	2.3×10^{6}	1.9×10^{1}	7.2	4.2×10^{6}	1.9×10^{6}
	$K_{eq}(3-2)^b$	6.7×10^{8}	3.6×10^{8}	1.6×10^{9}	8.6×10^{8}	1.3×10^{7}	2.3×10^{7}	4.6×10^{9}	7.7×10^{9}
	$k(2-1)^c$	6.3×10^{-29}	2.5×10^{-28}	6.7×10^{-33}	3.7×10^{-32}	5.2×10^{-29}	2.3×10^{-28}	6.8×10^{-41}	1.2×10^{-34}
	$k(1-3)^c$	2.1×10^{-33}	9.1×10^{-34}	2.6×10^{-35}	2.9×10^{-35}	2.7×10^{-35}	2.2×10^{-35}	1.7×10^{-36}	1.5×10^{-36}
	$k(2-3)^c$	1.1×10^{-55}	2.6×10^{-55}	2.1×10^{-56}	4.2×10^{-56}	6.3×10^{-58}	2.0×10^{-57}	1.8×10^{-60}	3.3×10^{-60}
Chloroform	$K_{eq}(1-2)^b$	3.8×10^{3}	1.6×10^{3}	3.0×10^{6}	1.0×10^{6}	3.5×10^{1}	8.8	2.2×10^{6}	8.4×10^{5}
	$K_{eq}(3-2)^b$	8.0×10^{7}	5.0×10^{7}	4.3×10^{8}	2.9×10^{8}	5.5×10^{6}	8.7×10^{6}	1.3×10^{9}	1.7×10^{9}
	$k(2-1)^c$	5.5×10^{-29}	2.0×10^{-28}	5.2×10^{-33}	2.6×10^{-32}	1.2×10^{-29}	6.2×10^{-29}	5.7×10^{-41}	8.9×10^{-35}
	$k(1-3)^c$	2.3×10^{-33}	6.9×10^{-34}	2.5×10^{-35}	2.0×10^{-35}	1.7×10^{-35}	1.1×10^{-35}	1.2×10^{-36}	9.1×10^{-37}
	$k(2-3)^c$	5.6×10^{-56}	9.0×10^{-56}	1.0×10^{-56}	2.0×10^{-56}	5.2×10^{-59}	2.1×10^{-58}	4.3×10^{-61}	1.1×10^{-60}
DMSO	$K_{eq}(1-2)^b$	3.2×10^{3}	1.4×10^{3}	4.2×10^{6}	1.3×10^{6}	9.0×10^{1}	1.6×10^{1}	2.9×10^{6}	9.0×10^{5}
	$K_{eq}(3-2)^b$	1.3×10^{7}	8.6×10^{6}	1.2×10^{8}	9.2×10^{7}	2.6×10^{6}	3.7×10^{6}	3.6×10^{8}	3.4×10^{8}
	$k(2-1)^c$	4.4×10^{-29}	1.6×10^{-28}	3.0×10^{-33}	1.4×10^{-32}	2.9×10^{-30}	2.0×10^{-29}	2.2×10^{-41}	6.6×10^{-35}
	$k(1-3)^c$	3.7×10^{-33}	3.6×10^{-34}	5.0×10^{-35}	3.0×10^{-35}	1.9×10^{-35}	1.1×10^{-35}	2.1×10^{-36}	1.3×10^{-36}
	$k(2-3)^c$	2.1×10^{-56}	3.3×10^{-56}	4.4×10^{-57}	8.8×10^{-57}	3.9×10^{-60}	2.6×10^{-59}	1.4×10^{-61}	4.2×10^{-61}

Notes: [a]All energetic data have been reported in kcal/mol. [b] $K_{eq}(n-m)$: the ratio of $[m]/[n]$, obtained from $K_{eq} = \exp(-\Delta G(n-m)/RT)$. [c] $k(n-m)$: the reaction rate for conversion of n to m.

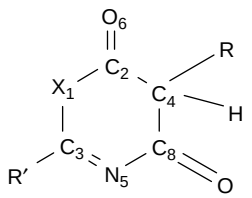

Figure 2. Numbering scheme for all tautomers and transition states.

was observed due to unfavourable spatial interaction at sp^3 carbon (C4) of tautomer **1** while in tautomer **2**, this carbon has sp^2 hybridisation and a planar structure. Moreover, all rate constants in these four molecules are smaller than those in the other molecules (**a**, **b**, **e** and **f**) that did not have the methyl substituent at the C4 position.

Rate constants of these conversions (obtained from barrier energies) are shown in the second part of Table 3. The barrier energies ($\Delta G^{\#}$) for the interconversion of tautomers are high and, following this, the corresponding reactions are carried out very slowly at room temperature. The difference between Gibbs free energies for TS1 and tautomer **2** ($\Delta G^{\#}(2-\text{ts1})$) lies between 54.9 and 71.6 kcal/mol, for TS2 and tautomer **1** ($\Delta G^{\#}(1-\text{ts2})$) lies between 62.4 and 66.6 kcal/mol and for TS3 and tautomer **2** ($\Delta G^{\#}(2-\text{ts3})$) lies between 91.1 and 98.4 kcal/mol. Therefore, all rate constants for the interconversion of tautomers are very low at room temperature. These data confirmed that, in both '1,3' and '1,5' hydrogen shifts, because of high energy barriers, the interconversion of tautomers is very slow at room temperature without using a catalyst or solvent assistance.

3.4 Solvation effect

Four different solvents (acetone, cyclohexane, chloroform and DMSO) with different dipole moments were used for computing free energies of solvation. Only aprotic solvents were employed in this part of study, so that the effects of protic solvents such as water were not considered, and the solvent-assisted tautomerism in the presence of water (as the protic solvent) will be discussed in Section 3.6. The results of these calculations are presented in Table 4. PCM calculations provide the total free energies of solvation, so the Gibbs free energies of compounds in the solvent can be obtained by this method.

As it is shown in Table 4, ΔG solvation for all optimised tautomers and transition states are negative and their values lie between -1.3 and -8.9 kcal/mol. These values were applied to calculate final ΔG between tautomers, $\Delta G^{\#}$ between each tautomer and the related transition state, and the rate and equilibrium constants of tautomerism in each solvent. For example, the maximum rate constant of tautomerism interconversion in all four solvents is $2.3 \times 10^{-28}\,s^{-1}$ and the maximum rate constant in the gas phase is $8.9 \times 10^{-28}\,s^{-1}$. Furthermore, in different solvents, the equilibrium constant between tautomers **1** and **2** ($K_{eq}(1-2)$) lies between 8.8 and 6.0×10^6 kcal/mol and between tautomers **2** and **3** ($K_{eq}(2-3)$) lies between 1.3×10^{-10} and 3.8×10^{-7} kcal/mol. Since the effect of the solvent on the stability of each structure (tautomer or transition state) is different, all equilibrium constants in solvents are different from those in the gas phase.

The diagram for the variation of ΔG solvation in each solvent vs. structures is shown in Figure 3 and the variation of ΔG solvation of each tautomer or transition state vs. solvents is shown in Figure 4. By observing Figure 3, it is easily seen that the order of the absolute amount of ΔG solvation is found to be acetone > DMSO > cyclohexane > chloroform. From Figure 4, tautomer **3** has the maximum absolute amount in ΔG solvation and

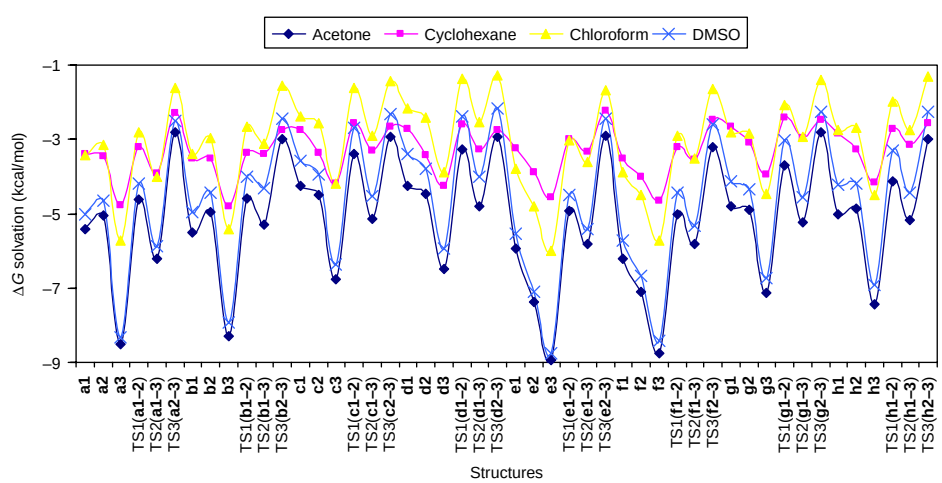

Figure 3. Variation of ΔG solvation in each solvent vs. all structures.

Downloaded At: 17:10 14 January 2011

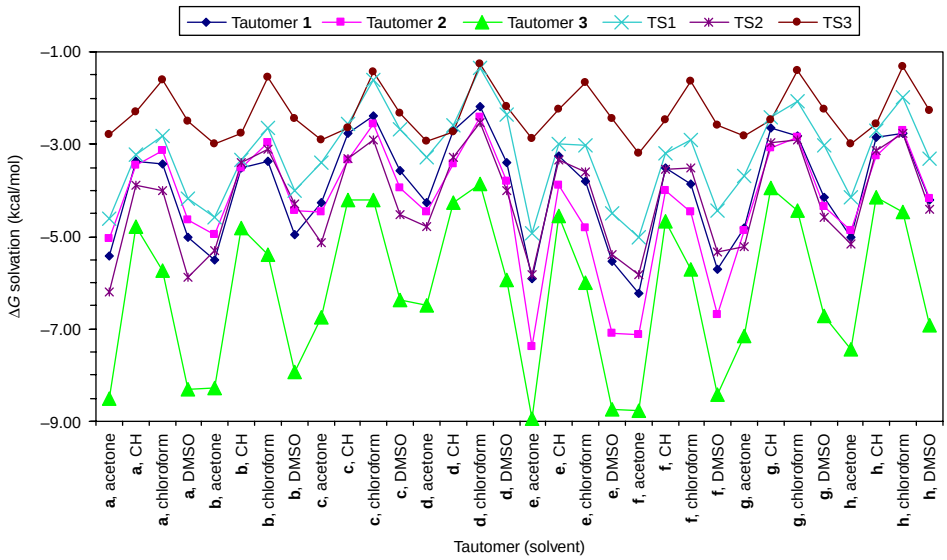

Figure 4. Variation of ΔG solvation in each tautomer or transition states. CH, cyclohexane.

TS3 and then TS2 have the minimum absolute amounts in ΔG solvation. The results of our PCM calculations show that this tautomerism interconversion is not effected extensively by the solvent. In other words, the equilibrium and rate constant in four different solvents (with different dipole moments) are comparable with those in the gas phase. This interconversion is very slow in both the gas phase and solvent.

3.5 *Frequencies*

In Table 5, some calculated frequencies of optimised structures are reported after correction by the scaling factor (see Section 2). The first column of Table 5 consists of C═O frequencies. In all structures except TS3, the value of this frequency is about 1700 cm^{-1}. In TS3, the order of the CO bond is between 1 and 2 and the frequency between 1387 and 1476 cm^{-1} is normal for this bond. C═N, C═C

Table 5. Most important frequencies (in cm^{-1}) of all structures.

Molecule	C═O	C═N	C═C	O—H	Molecule	C═O	C═N	C═C	O—H
a1	1747	1568	–	–	**e1**	1814	1602	–	–
a2	1708	1501	1588	3626	**e2**	1779	1535	1593	3669
a3	1670	1534	1600	3640.8	**e3**	1700	1564	1653	3675
TS1(**a1**–**2**)	1756	1484	1508	1825	TS1(**e1**–**2**)	1831	1532	1514	1802
TS2(**a1**–**3**)	1708	1589	1436	1746	TS2(**e1**–**3**)	1733	1631	1536	1779
TS3(**a2**–**3**)	1449	1541	1397	1747	TS3(**e2**–**3**)	1476	1582	1438	1745
b1	1741	1598	–	–	**f1**	1806	1620	–	–
b2	1703	1520	1591	3628	**f2**	1772	1594	1546	3671
b3	1669	1546	1616	3643	**f3**	1700	1662	1579	3676
TS1(**b1**–**2**)	1749	1523	1491	1829	TS1(**f1**–**2**)	1821	1542	1514	1806
TS2(**b1**–**3**)	1708	1622	1429	1754	TS2(**f1**–**3**)	1733	1659	1529	1783
TS3(**b2**–**3**)	1447	1581	1390	1754	TS3(**f2**–**3**)	1470	1624	1432	1748
c1	1738	1568	–	–	**g1**	1806	1601	–	–
c2	1676	1512	1586	3633	**g2**	1762	1551	1627	3638
c3	1654	1538	1591	3646	**g3**	1684	1571	1649	3674
TS1(**c1**–**2**)	1732	1508	1473	1834	TS1(**g1**–**2**)	1806	1540	1483	1752
TS2(**c1**–**3**)	1692	1584	1417	1766	TS2(**g1**–**3**)	1713	1626	1517	1787
TS3(**c2**–**3**)	1416	1542	1391	1753	TS3(**g2**–**3**)	1466	1583	1415	1748
d1	1732	1597	–	–	**h1**	1798	1618	–	–
d2	1673	1531	1592	3632	**h2**	1756	1564	1627	3637
d3	1656	1606	1551	3647	**h3**	1689	1589	1652	3674
TS1(**d1**–**2**)	1726	1531	1477	1838	TS1(**h1**–**2**)	1794	1551	1496	1812
TS2(**d1**–**3**)	1696	1615	1410	1773	TS2(**h1**–**3**)	1716	1650	1509	1789
TS3(**d2**–**3**)	1387	1580	1300	1756	TS3(**h2**–**3**)	1463	1625	1412	1750

Note: All frequencies have been reported after correction by the scaling factor.

Downloaded At: 17:10 14 January 2011

Table 6. Comparison between computational and experimental IR frequencies (in cm^{-1}).

	Average of computed frequencies	Average of this frequency for reference compounds	% Error
X═S			
C═O	1707	1618	5.2
C═N	1555	1582	1.7
O—H	3422	3188	6.9
X═O			
C═O	1761	1741	1.1
C═N	1592	1610	1.1
O—H	3452	3220	6.7

and O—H frequencies are reported, respectively, in the second, third and fourth columns of Table 5.

All of these calculated frequencies are in accordance with the same frequency in similar compounds. To prove this claim, calculated frequencies have been compared with experimental frequencies (extracted from [14]) and the results are shown in Table 6. The data reported in this table show that our computational frequencies are comparable with experimental frequencies and the maximum value of calculation error is 6.9%. These frequency data and their comparisons with the experiments show the potency of our method to use it instead of experiment (which will be more expensive) for the determination of molecular and spectral parameters. Hence, IR calculations were used for the cross-validation of the calculated tautomers with the experiments.

Table 7. Final structure of optimised tautomers and transition states in the presence of one, two and three water molecules.

Molecule	One water molecule	Two water molecules	Three water molecules
e1	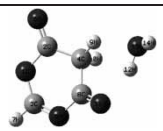	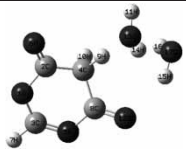	
TS1(**e1**–**2**)	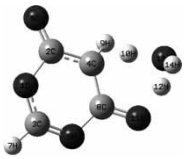	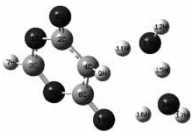	
e2	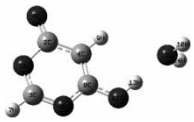		
TS2(**e2**–**3**)	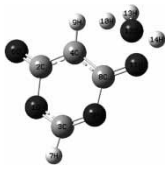		
e3		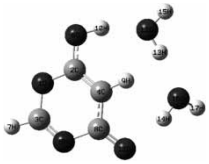	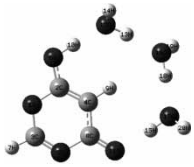

Downloaded At: 17:10 14 January 2011

Downloaded At: 17:10 14 January 2011

Table 8. Corrected kinetic and thermodynamic data of molecule **1** in the presence of one, two and three water molecules at B3LYP/6-311++G** level of theory[a].

Number of water molecules	$\Delta H(1-2)^b$	$\Delta H(3-2)^b$	$\Delta G(1-2)^c$	$\Delta G(3-2)^c$	$K_{eq}(1-2)^d$	$K_{eq}(3-2)^d$	$\Delta G^{\#}(2-\text{ts1})^e$	$\Delta G^{\#}(2-\text{ts3})^e$	$k(2-1)^f$	$k(2-3)^f$
0	−1.6	−10.6	−1.1	−10.4	6.5	4.2×10^{7}	55.1	93.8	2.4×10^{-28}	1.0×10^{-56}
1	−5.1	−9.6	−4.9	−9.3	3.8×10^{3}	6.6×10^{6}	32.9	34.5	4.5×10^{-12}	3.2×10^{-13}
2	−11.1	−7.2	−7.8	−7.6	4.9×10^{5}	3.6×10^{5}	23.8	20.2	2.2×10^{-5}	1.0×10^{-2}
3	−15.1	−6.6	−14.6	−6.9	5.1×10^{10}	1.2×10^{5}	21.2	17.6	1.8×10^{-3}	7.3×10^{-1}

Notes: [a]All ΔH and ΔG values were reported in kcal/mol and rate constants were reported in s^{-1}. [b] $\Delta H(n-m)$ = Enthalpy of tautomer $m(Hm)$ − Enthalpy of tautomer $n(Hn)$. [c] $\Delta G(n-m)$ = Gibbs free energy of tautomer $m(Gm)$ − Gibbs free energy of tautomer $n(Gn)$. [d] $K_{eq}(n-m)$: the ratio of $[m]/[n]$, obtained from $K_{eq} = \exp(-\Delta G(n-m)/RT)$. [e] $\Delta G^{\#}(n-\text{ts1})$ = Gibbs free energy of ts1 (Gts1) − Gibbs free energy of tautomer $n(Gn)$. [f] $k(n-m)$: the reaction rate for conversion of n to m.

3.6 Water-assisted tautomerism

Intermolecular tautomerism of molecule **e** in the presence of one, two and three water molecules was studied at the B3LYP/6-311++G** level of theory. The optimised structures are shown in Table 7 and kinetic and thermodynamic results of these calculations are listed in Table 8.

The data reported in Table 8 show that the values of $\Delta G(1-2)$ for molecule **e** are −1.1, −4.9, −7.8 and −14.6 kcal/mol, respectively, in the gas phase and with one, two and three water molecules. These data show that the effect of water molecules on the stability of tautomer **2** is more than that for tautomer **1**. Moreover, $\Delta G(3-2)$ values are −10.4, −9.3, −7.6 and −6.9 kcal/mol, respectively, in the gas phase and with one, two and three water molecules.

The kinetic effects of water-assisted tautomerism are more profound than thermodynamic effects. All water-assisted tautomerism rate constants are higher than simple tautomerism rate constants. For example, the rate constant for the conversion of **e2** to **e1** ($k(2-1)$) from 2.4×10^{-28} in the absence of water (in the gas phase) goes up to 4.5×10^{-12}, 2.2×10^{-5} and 1.8×10^{-3}, respectively, with one, two and three water molecules. In addition, the rate constant for the conversion of **e2** to **e3** ($k(2-3)$) from 1.0×10^{-56} in the absence of water (in the gas phase) goes up to 3.2×10^{-13}, 1.0×10^{-2} and 7.3×10^{-1}, respectively, with one, two and three water molecules. Finally, activation barriers in the presence of water molecules are in general lower than those in the gas phase.

4. Conclusion

In this work, DFT calculations have been applied to the study of structures, molecular parameters and vibrational frequencies of three possible tautomers of some OZDs and TZDs using the B3LYP/6-311++G** level of theory. Calculated frequencies show good agreement with the experiment. Moreover, kinetic and thermodynamic behaviour of these tautomeric interconversions in the gas phase have been studied. In all structures, tautomer **2** is most stable and tautomer **3** is least stable. Optimisation of structures in four different solvents (acetone, chloroform, DMSO and cyclohexane) has been investigated and the results show a little difference between the gas and solvent calculations. In addition, the tautomerism interconversion in the presence of one, two and three water molecules has been studied. The results show that, although the simple interconversion of tautomers is very slow, it can be done faster in the presence of water molecules. All reaction rate constants are increased by increasing the number of water molecules near the tautomers.

Acknowledgements

We are grateful to my sincere friends, Prof. Hassan Sabzyan, Prof. Jahangir Emrani and Dr Hassan Sheybani, for their valuable assistance. This work was supported by the research affairs of the University of Zabol.

References

[1] N. Benaamane, B. Nedjar-Kolli, Y. Bentarzi, L. Hammal, A. Geronikaki, P. Eleftheriou, and A. Lagunin, *Synthesis and* in silico *biological activity evaluation of new N-substituted pyrazolo-oxazin-2-one systems*, Bioorg. Med. Chem. 16 (2008), pp. 3059–3066.

[2] M.E. Pierce, R.L. Parsons, L.A. Radesca, Y.S. Lo, S. Silvermon, J.R. Oore, Q. Islam, A. Chaodhury, J.M.D. Fortunak, D. Nguyen, C. Luo, S.F. Morgan, W.P. Davis, P.N. Confalone, C. Chen, R.D. Tillyer, L. Frey, L. Tan, F. Xu, D. Zhao, A.S. Thompson, E.G. Corley, E.J.J. Grabowski, R. Reamer, and P.J. Reider, *Practical asymmetric synthesis of efavirenz (DMP 266), an HIV-1 reverse transcriptase inhibitor*, J. Org. Chem. 63 (1998), pp. 8536–8543.

[3] J.C. Kern, E.A. Terefenko, A. Fensome, R. Unwalla, J. Wrobel, Y. Zhu, J. Cohen, R. Winneker, Z. Zhang, and P. Zhang, *SAR studies of 6-(arylamino)-4,4-disubstituted-1-methyl-1,4-dihydro-benzo[d][1,3]oxazin-2-ones as progesterone receptor antagonists*, Bioorg. Med. Chem. Lett. 17 (2007), pp. 189–192.

[4] A. Bolognese, G. Correale, M. Manfra, A. Lavecchia, O. Mazzoni, E. Novellino, V. Barone, P. La Colla, and R. Loddo, *Antitumor agents. 3. Design, synthesis, and biological evaluation of new pyridoisoquinolindione and dihydrothienoquinolindione derivatives with potent cytotoxic activity*, J. Med. Chem. 45 (2002), pp. 5217–5220.

[5] R.L. Jarvest, S.C. Connor, J.G. Gorniak, L.J. Jennings, H.T. Serafinowska, and A. West, *Potent selective thienoxazinone inhibitors of herpes proteases*, Bioorg. Med. Chem. Lett. 7 (1997), pp. 1733–1736.

[6] P.W. Hsieh, T.L. Hwang, C.C. Wu, F.R. Chang, T.W. Wang, and Y.C. Wu, *The evaluation of 2,8-disubstituted benzoxazinone derivatives as anti-inflammatory and anti-platelet aggregation agents*, Bioorg. Med. Chem. Lett. 15 (2005), pp. 2786–2792.

[7] K. Waisser, J. Gregor, L. Kubikova, V. Klimesova, J. Kunes, M. Machacck, and J. Kaustova, *New groups of antimycobacterial agents: 6-Chloro-3-phenyl-4-thioxo-2H-1,3-benzoxazine-2(3H)-ones and 6-chloro-3-phenyl-2H-1,3-benzoxazine-2,4(3H)-dithiones*, Eur. J. Med. Chem. 35 (2000), pp. 733–737.

[8] P.W. Hsieh, F.R. Chang, C.H. Chang, P.W. Cheng, L.C. Chiang, F.L. Zeng, K.H. Lin, and Y.C. Wu, *Two new protopines argemexicaines A and B and the anti-HIV alkaloid 6-acetonyldihydrochelerythrine from formosan Argemone mexicana*, Bioorg. Med. Chem. Lett. 14 (2004), pp. 4751–4757.

[9] G.R. Madhavan, R. Chakrabarti, K.A. Reddy, B.M. Rajesh, V. Balaju, P.B. Rao, R. Rajagopalan, and J. Iqbal, *Dual PPAR-α and -γ activators derived from novel benzoxazinone containing thiazolidinediones having antidiabetic and hypolipidemic potentia*, Bioorg. Med. Chem. 14 (2006), pp. 584–589.

[10] K. Afarinkia, A. Bahar, J. Neuss, and A. Ruggiero, *2(H)-1,4-Oxazin-2-ones as ambident azadienes*, Tetrahedron Lett. 45 (2004), pp. 3995–3999.

[11] B.P. Medaer and G.J. Hoornaert, *Synthesis of new 1H-imidazoles via reactions of 3(,5)-(di)chloro-2H-1,4-(benz)oxazin-2-ones with α-aminoketones*, Tetrahedron 55 (1999), pp. 3987–3991.

[12] O. Myata, M. Namba, M. Ueda, and T. Naito, *A novel synthesis of amino-1,2-oxazinones as a versatile synthon for β-lactams*, Org. Biomol. Chem. 2 (2004), pp. 1274–1278.

[13] K. Kandasamy, H.B. Singh, R.J. Butcher, and J.P. Jasinski, *Synthesis, structure and catalytic properties of VIV, MnIII, MoVI, and UVI complexes containing bidentate (N, O) oxazine and oxazoline ligands*, Inorg. Chem. 43 (2004), pp. 5704–5713.

[14] H. Sheibani, M.H. Mosslemin, S. Behzadi, M.R. Islami, H. Foroughi, and K. Saidi, *A simple and an efficient approach to the synthesis of a specific tautomer of 1,3-thiazinones and 1,3-oxazinones*, ARKIVOC xv (2005), pp. 88–96.

[15] M.M. Abdulla, *Anti-inflammatory activity of heterocyclic systems using abietic acid as starting material*, Monatsh. Chem. 139 (2008), pp. 697–705.

[16] M.V. Vovk, A.V. Bol'but, P.S. Lebed, and V.I. Boiko, *1,1-Dichloro-2,2,2-trihaloethyl isocyanates and N-(1-chloro-2,2,2-trihaloethylidene)urethanes in the synthesis of 4-trihalomethyl-2H-1,3-benzoxazin-2-ones*, Chem. Heterocycl. Compd. 40 (2004), pp. 101–105.

[17] C. Lamberth and F. Querniard, *First synthesis and further functionalization of 7-chloro-imidazo[2,1-b][1,3]thiazin-5-ones*, Tetrahedron Lett. 49 (2008), pp. 2286–2288.

[18] O. Arjona, A.G. Csaky, M.C. Murcia, and J. Plumet, *The Staudinger reaction of imines derived from 7-oxanorbornenone: Formation of spiranic oxazinone versus lactam rings*, Tetrahedron Lett. 43 (2002), pp. 6405–6409.

[19] V.K. Redd, H. Miyabe, M. Yamauchi, and Y. Takemoto, *Enantioselective synthesis of [1,2]-oxazinone scaffolds and [1,2]-oxazine core structures of FR900482*, Tetrahedron 64 (2008), pp. 1040–1048.

[20] P. Gizecki, R.A. Youcef, C. Poulard, R. Dhal, and G. Dujardin, *Diastereoselective preparation of novel tetrahydrooxazinones via heterocycloaddition of N-Boc, O-Me-acetals*, Tetrahedron Lett. 45 (2004), pp. 9589–9594.

[21] S. Simonyiova and K.T. Wanner, *Electrocyclic ring-opening reactions may cause failure of enolate alkylation of 1,4-oxazin-2-one based chiral glycine equivalents*, Tetrahedron 64 (2008), pp. 5107–5112.

[22] F. Uehara, M. Sato, C. Kaneko, and H. Kurihara, *The effect of a para substituent on the conformational preference of 2,2-diphenyl-1,3-dioxanes: Evidence for the anomeric effect from X-ray crystal structure analysis*, J. Org. Chem. 64 (1999), pp. 1436–1441.

[23] A. Abouelfida, J.C. Roze, J.P. Pradere, and M. Jubault, *Selective reduction of substituted 4H-1,3-thiazin-4-ones*, Phosphorus, Sulfur Silicon Relat. Elem. 54 (1990), pp. 123–134.

[24] A. Hamdach, R.J. Zaragozá, E. Zaballos-García, and J. Sepúlveda-Arques, *Quantitative ring contraction of 5-hydroxy-1,3-oxazin-2-ones into 5-hydroxymethyl-1,3-oxazolidin-2-ones: A DFT study*, Theochem 806 (2007), pp. 141–144.

[25] G. Song, F. Xing, X. Qu, J.B. Chaires, and J. Ren, *Oxazine 170 induces DNA:RNA:DNA triplex formation*, J. Med. Chem. 48 (2005), pp. 3471–3473.

[26] G. Alagona and C. Ghio, *Keto–enol tautomerism in linear and cyclic beta-diketones: A DFT study* in vacuo *and in solution*, Int. J. Quantum Chem. 108 (2008), pp. 1840–1855.

[27] N.V. Belova, H. Oberhammer, G.V. Girichev, and S.A. Shlykov, *Tautomeric properties and gas-phase structure of 3-chloro-2,4-pentanedione*, J. Phys. Chem. A 112 (2008), pp. 3209–3214.

[28] B.I. Buzykin, E.V. Mronova, V.N. Nabiullin, N.M. Azancheev, L.V. Awakumova, I.K. Rizvanov, A.T. Gubaiduffin, I.A. Litvinov, and V.V. Syakaev, *Tautomerism of aza cycles: II. Synthesis and structure of 5-substituted 3-(2-hydroxyethylsulfanyl)-1H-1,2,4-triazoles and their salts. Preference of the 1H,4H-1,2,4-triazolium tautomers*, Russ. J. Gen. Chem. 78 (2008), pp. 461–479.

[29] A. Brenlla, F. Rodriguez-Prieto, M. Mosquera, M.A. Rios, and M.C.R. Rodriguez, *Solvent-modulated ground-state rotamerism and tautomerism and excited-state proton-transfer processes in o-hydroxynaphthylbenzimidazoles*, J. Phys. Chem. A 113 (2009), pp. 56–67.

[30] Y.M. Guo and B.Z. Li, *A theoretical study on tautomerism of 2-mercaptobenzimidazole and its analogues*, Acta Chim. Sin. 65 (2007), pp. 1561–1567.

[31] G.A. Chmutova, E.R. Ismagilova, and G.A. Shamov, *Quantum-chemical study of the structure and reactivity of pyrazol-5-ones and their thio and seleno analogs: X. 1-Methylpyrazol-5-one and its thio and seleno analogs in H-complex formation reactions in the gas phase and in solutions*, Russ. J. Gen. Chem. 77 (2007), pp. 1628–1634.

[32] V. Enchev and S. Angelova, *Does tautomeric equilibrium exist in 4-nitroso-5-pyrazolones?* Theochem 897 (2009), pp. 55–60.

[33] A.P. Fu, H.L. Li, and D.M. Du, *Thiol–thione tautomerism in 2-pyridinethione: Effect of hydration*, Theochem 767 (2006), pp. 51–60.

Downloaded At: 17:10 14 January 2011

[34] V. Bertolasi, P. Gilli, and G. Gilli, *Crystal chemistry and prototropic tautomerism in 2-(1-iminoalkyl)-phenols (or naphthols) and 2-diazenyl-phenols (or naphthols)*, Curr. Org. Chem. 13 (2009), pp. 250–268.
[35] C. Chatgilialoglu, C. Caminal, A. Altieri, G.C. Vougioukalakis, Q.G. Mulazzani, T. Gimisis, and M. Guerra, *Tautomerism in the guanyl radical*, J. Am. Chem. Soc. 128 (2006), pp. 13796–13805.
[36] P.T. Chou, G.R. Wu, C.Y. Wei, M.Y. Shiao, and Y.I. Liu, *Excited-state double proton transfer in 3-formyl-7-azaindole: Role of the $n\pi^*$ state in proton-transfer dynamics*, J. Phys. Chem. A 104 (2000), pp. 8863–8871.
[37] R. Dobosz, E. Kolehmainen, A. Valkonen, B. Osmiaowski, and R. Gawinecki, *Tautomeric preferences of phthalones and related compounds*, Tetrahedron 63 (2007), pp. 9172–9178.
[38] N.E.A. El-Gamel, L. Seyfarth, J. Wagler, H. Ehrenberg, M. Schwarz, J. Senker, and E. Kroke, *The tautomeric forms of cyameluric acid derivatives*, Chem. Eur. J. 13 (2007), pp. 1158–1173.
[39] C.F. Rodiquez, A. Cunje, T. Shoeib, I.K. Chu, A.C. Hopkinson, and K.W.M. Siu, *Solvent-assisted rearrangements between tautomers of protonated peptides*, J. Phys. Chem. A 104 (2000), pp. 5023–5028.
[40] M. Amedjkouh, *Primary amine catalyzed direct asymmetric aldol reaction assisted by water*, Tetrahedron: Asymmetry 16 (2005), pp. 1411–1414.
[41] X.Q. Liang, W.X. Zheng, N.B. Wong, Y.J. Shu, and A.M. Tian, *Solvent-assisted catalysis mechanism on keto–enol tautomerism of cyameluric acid*, Theochem 732 (2005), pp. 127–137.
[42] A. Bhan, Y.V. Joshi, W.N. Delgass, and K.T. Thomson, *DFT investigation of alkoxide formation from olefins in H-ZSM-5*, J. Phys. Chem. B 107 (2003), pp. 10476–10482.
[43] X. Rozanska, R.A.V. Santen, T. Demuth, F. Hutschka, and J. Hafner, *Benchmark data for interactions in zeolite model complexes and their use for assessment and validation of electronic structure methods*, J. Phys. Chem. B 107 (2003), pp. 1309–1313.
[44] A.D. Becke, *Density-functional thermochemistry. III. The role of exact exchange*, J. Chem. Phys. 98 (1993), pp. 5648–5654.
[45] T.C. Lee, W.T. Yang, and R.G. Parr, *Density-functional crystal orbital study on the structures and energetics of polyacetylene isomers*, Phys. Rev. B 37 (1988), pp. 785–789.
[46] B.G. Johnson, P.M.W. Gill, and J.A. Pople, *The performance of a family of density functional methods*, J. Chem. Phys. 98 (1993), pp. 5612–5617.
[47] C.W. Bauschlicher and H. Partridge, *A modification of the Gaussian-2 approach using density functional theory*, J. Chem. Phys. 103 (1995), pp. 1788–1795.
[48] M.J. Frisch, *Gaussian 03, Revision C02*, Gaussian Inc., Wallingford, CT, 2004.
[49] R. Dennington, T. Keith, J. Millam, K. Eppinnett, W.L. Hovell, and R. Gilliland, *GaussView, version 3.09*, Semichem Inc., Shawnee Mission, KS, 2003.
[50] C. Peng, P.Y. Ayala, H.B. Schlegel, and M.J. Frisch, *Using redundant internal coordinates to optimize geometries and transition states*, J. Comp. Chem. 17 (1996), p. 49.
[51] C. Peng and H.B. Schlegel, *Combining synchronous transit and quasi-Newton methods to find transition states*, Israel J. Chem. 33 (1994), p. 449.
[52] R.I. Masel, *Chemical Kinetics and Catalysis*, Wiley-Interscience, New York, 2001.
[53] K.A. Holbrook, M.J. Pilling, and S.H. Robertson, *Unimolecular Reactions*, Wiley, New York, 1996.
[54] G. Gilbert and S.C. Smith, *Theory of Unimolecular and Recombination Reactions*, Blackwell, Oxford, 1990.
[55] S. Mietrus and E. Scrocco, *Correlation of observed and model vibrational frequencies for aqueous organic acids*, J. Chem. Phys. 55 (1981), pp. 117–122.
[56] S. Mietrus and E. Tomasi, *Computational study of proton binding at the rutile/electrolyte solution interface*, J. Chem. Phys. 65 (1981), pp. 239–244.

Downloaded At: 17:10 14 January 2011